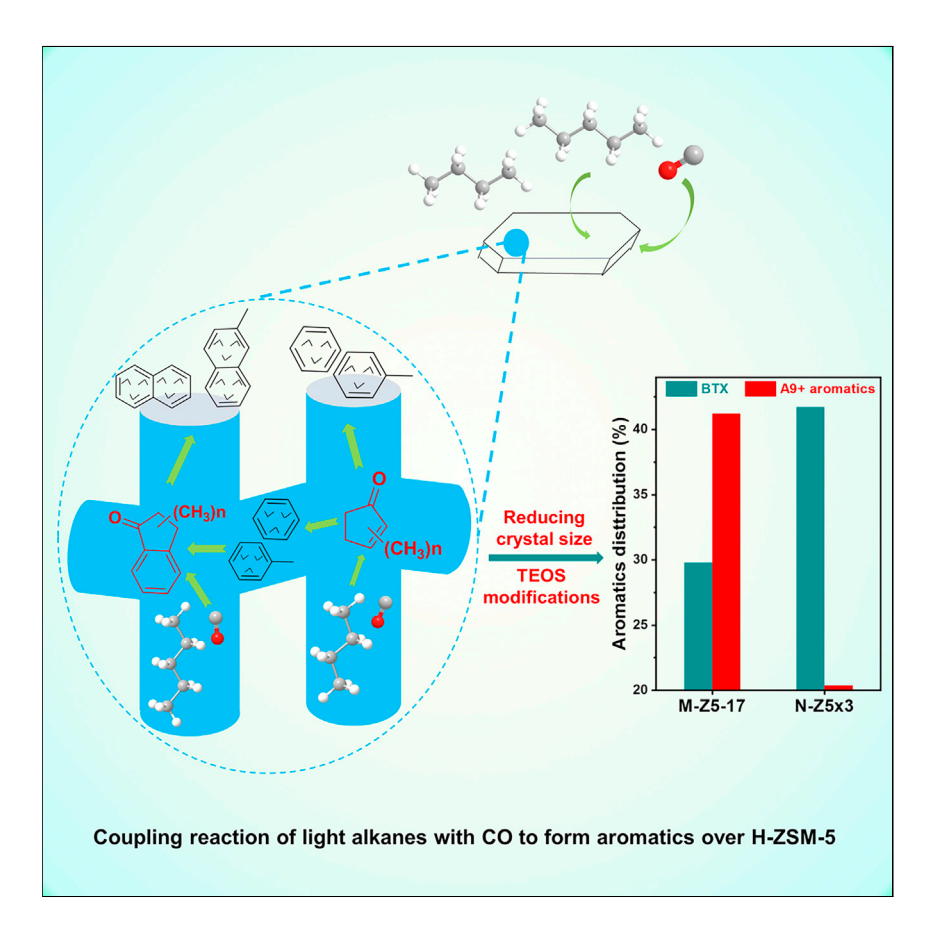


### **Article**

Aromatization mechanism of coupling reaction of light alkanes with CO over acidic zeolites: Cyclopentenones as key intermediates



The introduction of CO into light alkanes over H-ZSM-5 significantly enhances aromatic formation, and high aromatics selectivity could be achieved. The key intermediates, such as methyl-substituted cyclopentenones and indanones, are observed on the reacted zeolites and could be converted into BTX and heavy aromatics, respectively. The formation and evolution route of these intermediates are clarified, and the coupling mechanism is proposed. According to this, using nano-size ZSM-5 and TEOS modifications significantly improves the BTX selectivity during the coupling reaction.



Changcheng Wei, Jinzhe Li, Kuo Yang, Qijun Yu, Shu Zeng, Zhongmin Liu

liuzm@dicp.ac.cn

### Highlights

High aromatic selectivity is achieved by coupling light alkanes with CO over H-ZSM-5

Key intermediates are observed, and their formation and evolution route are clarified

The complete mechanism for coupling reaction of light alkanes with CO is proposed

Nano-sized ZSM-5 and TEOS modifications are applied to improve the BTX selectivity

Wei et al., Chem Catalysis 1, 1273–1290 November 18, 2021 © 2021 Elsevier Inc. https://doi.org/10.1016/j.checat.2021.09.004





### **Article**

# Aromatization mechanism of coupling reaction of light alkanes with CO over acidic zeolites: Cyclopentenones as key intermediates

Changcheng Wei, 1,2 Jinzhe Li, 1 Kuo Yang, 1 Qijun Yu, 1 Shu Zeng, 1,2 and Zhongmin Liu 1,2,3,\*

#### **SUMMARY**

The aromatization of light alkanes ( $C_4$ - $C_6$ ) is an important value-added reaction. However, the yield of aromatics is always limited by the simultaneous generation of small alkanes (CH<sub>4</sub> and C<sub>2</sub>H<sub>6</sub>) due to H/C balance. Herein, we demonstrate that the introduction of CO into light alkanes over zeolites significantly enhanced aromatic selectivity and an aromatics selectivity of 85% was achieved in the case of cyclopentane and CO coupling reaction over H-ZSM-5. Methyl-substituted cyclopentenones were observed and considered as the most important intermediates for aromatics formation. Multiple characterizations revealed the coupling mechanism: (1) CO inserts into carbenium ions to form acylium cations, (2) acylium cations react with olefins to generate unsaturated ketones, (3) unsaturated ketones cyclize to methylsubstituted cyclopentenones, (4) methyl-substituted cyclopentenones convert to monocytic aromatics. Methyl-substituted indanones were also discovered causing the generation of binuclear aromatics, such as naphthalene. Nano-sized ZSM-5 and TEOS modifications were applied to enhance the BTX selectivity.

#### **INTRODUCTION**

Aromatic hydrocarbons, widely employed in the production of plastic, pesticide, dye, solvent, adhesives, etc.  $^{1,2}$  are the most significant and fundamental building blocks in the chemical industry, with 2%–6% annually growing demand globally.  $^3$  Currently, aromatics such as benzene, toluene, and xylenes (BTX) are mainly generated from catalytic reforming of naphtha over noble metal catalysts  $^4$  such as Re-Pt/  ${\rm Al}_2{\rm O}_3^{5,6}$  in the presence of hydrogen. In principle, straight-chain alkanes such as n-hexane and light alkanes (C < 6) in naphtha feedstock are difficult to be transformed into aromatics in this process.

Straight-chain alkanes could be converted into aromatics over Pt clusters supported on nonacidic materials such as KL zeolites.  $^{7,8}$  To improve the catalytic activity and stability of this type of Pt-based catalysts, tremendous amounts of research had concentrated on the modification of the dispersion and electronic state of Pt by the introduction of promoters such as Fe,  $^{9,10}$  Zn,  $^{11}$  and Co.  $^{12}$  Catalyst carriers were also modified to obtain a better yield of aromatics.  $^{13-15}$  The aromatization of straight-chain alkanes over these catalysts followed 1,6-ring closure mechanisms,  $^{15}$  according to which, light alkanes (C < 6), widely generated as byproducts in the chemical industries, were also difficult to be transformed into aromatics.

Zeolites modified by metals, such as  $Zn^{16-20}$  and  $Ga^{21-24}$  through impregnation, ion exchange, physical mixing, etc., were widely employed for the aromatization of light

### The bigger picture

Light alkanes ( $C_4$ - $C_6$ ) could be widely derived from refinery industry as byproducts, and the aromatization of light alkanes is an important value-added reaction. However, light alkanes had a higher hydrogen to carbon (H/C) ratio than that of aromatics from the perspective of element composition, so the yield of aromatics is always limited by the simultaneous generation of small alkanes (CH<sub>4</sub> and C<sub>2</sub>H<sub>6</sub>) due to H/ C balance requirement of the reaction. According to this, we expect that hydrogen-deficient substances, such as CO, are introduced into light alkane conversion to balance the excess hydrogen of alkanes. We indeed observe that the introduction of CO into light alkane over acidic zeolites could tune the H/C ratio of products and high aromatic selectivity could be achieved. Considering the large existing supply capacities of CO and light alkanes, the coupling reaction might have great potential for industrial applications.





alkanes (C < 6), which could improve the aromatic selectivity via promoting the dehydrogenation of alkanes. Nevertheless, these catalysts after reaction suffered from the inevitable and unrecoverable change, including metal evaporation, segregation, and aggregation, which accounted for the reduction of catalytic activity and the difficulty in regeneration of the catalyst.  $^{25,26}$ 

From the perspective of element composition, light alkanes have a higher hydrogen to carbon (H/C) ratio than that of aromatics. Therefore, redundant hydrogen needs to be removed for the aromatization of these light alkanes. Our previous work reported that hydrogen-deficient substances, such as CO, were introduced into n-hexane conversion to balance the excess hydrogen of n-hexane, demonstrating that the H/C ratio of products could be tuned and a high aromatic selectivity could be achieved. However, the reaction mechanisms are still not clear, such as how CO participates in the coupling reaction and what the reaction intermediate and its formation and evolution mechanism is, etc. Moreover, although we discovered that there is a coupling effect between n-hexane with CO, whether there exists a coupling effect between light alkanes (C < 6) with CO is also very interesting and meaningful, because catalytic reforming of these alkanes is very difficult and there is still no effective process for the aromatization of light alkanes in the viewpoint of industrial application.

Zeolites are the potential catalysts for the coupling conversion. In particular, H-ZSM-5 possesses a three-dimensional ten-ring channel system with channel size (0.55 nm) close to the kinetic diameter of BTX, considered to be a suitable catalyst for production of aromatics.  $^{20,25,28}$  Herein, we systematically investigated the coupling reaction of light alkanes (C<sub>4</sub>-C<sub>6</sub>) with CO over acidic zeolites. *In situ* diffuse reluctance infrared fourier transform (DRIFT) study, *in situ* UV-vis characterizations, and  $^{13}\text{C}$  solid-state NMR were meticulously designed to reveal the mechanism of the generation of aromatics. Nano-sized ZSM-5 and tetraethoxysilane (TEOS) modifications were employed to enhance the BTX selectivity, which further verified the proposed mechanism for the coupling reactions.

### **RESULTS AND DISCUSSION**

#### The coupling conversion of CO and different light alkanes

Different light alkanes, such as n-butane,  $C_5$  alkanes with different skeleton structures, and n-hexane, were employed to evaluate the coupling reactions over micro-sized H-ZSM-5. As shown in Figures 1A and S1A, a considerably higher selectivity to aromatics (including BTX and  $A_{9+}$  aromatics) was observed for n-pentane, cyclopentane, and isopentane conversion in CO than that in He. Simultaneously, the introduction of CO resulted in the significant decrease of small alkanes (Figure S1B). These results were different from the generation of aromatics via hydrogen transfer reaction, which causes the simultaneous formation of small alkanes, indicating the strong coupling effect between these light alkanes and CO. The aromatic selectivity for the coupling cyclopentane with CO was higher than that of the other two alkanes, because the H/C ratio of cyclopentane (2) was lower than that of n-pentane (2.4) and isopentane (2.4), implying that less hydrogen is needed to be removed during cyclopentane conversion to aromatics. Under optimized reaction conditions, an astounding aromatic selectivity of 85% was achieved for the coupling of cyclopentane with CO (Figure 1B).

Figure 1C shows that, with increasing carbon number of n-alkanes (from  $C_4$  to  $C_6$ ), the aromatic selectivity gradually increased and the alkane selectivity decreased,

<sup>1</sup>National Engineering Laboratory for Methanol to Olefins, Dalian National Laboratory for Clean Energy, Dalian Institute of Chemical Physics, Chinese Academy of Sciences, Dalian 116023, Liaoning, China

<sup>2</sup>University of Chinese Academy of Sciences, Beijing 100049, China

<sup>3</sup>Lead contact

\*Correspondence: liuzm@dicp.ac.cn https://doi.org/10.1016/j.checat.2021.09.004



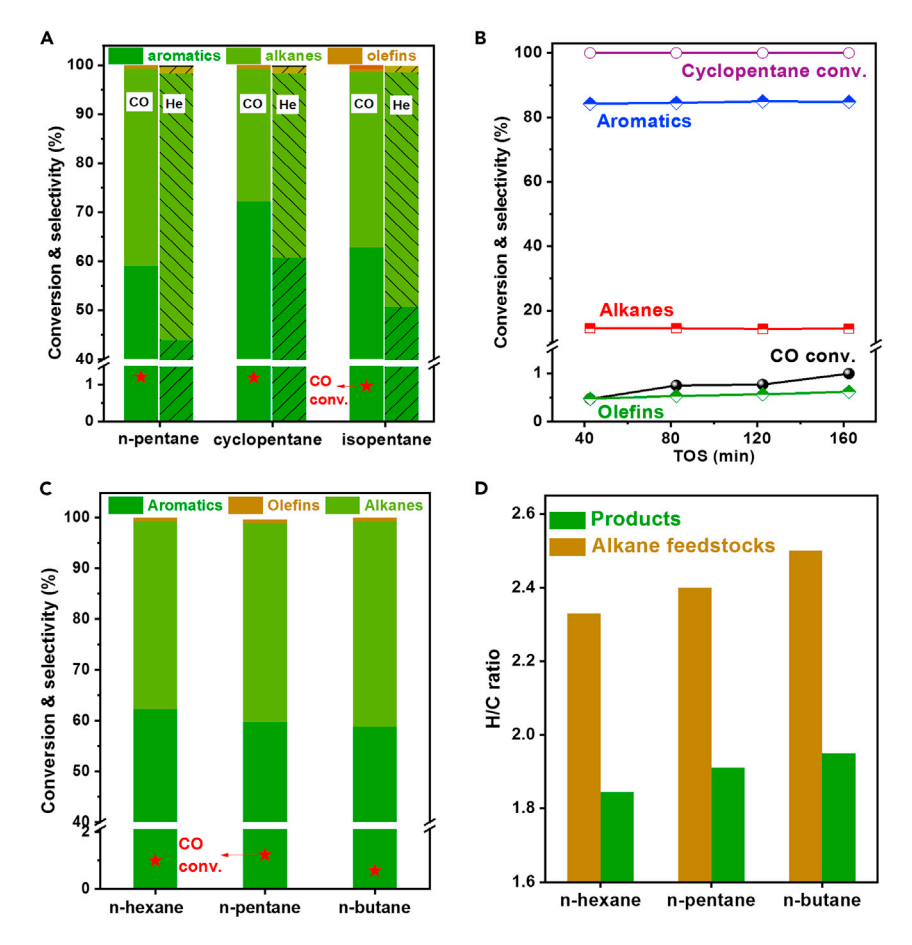


Figure 1. Catalytic performance for the conversion of different alkanes in He or CO atmospheres (A) Comparison of CO conversion and the products distribution for the conversion of n-pentane, cyclopentane, and isopentane in He or CO atmospheres. Reaction conditions: 0.4 g M-Z5-17, T =  $450^{\circ}$ C,  $P_{alkanes} = 24$  kPa,  $P_{((CO+Ar) \text{ or He})} = 2,976$  kPa, total flow = 40 mL/min at standard temperature and pressure (STP), TOS = 1.4 h.

(B) Catalytic performance for coupling reaction of cyclopentane with CO under optimized conditions. Reaction conditions: 0.4 g M-Z5-17, T =  $500^{\circ}$ C,  $P_{cyclopentane} = 10$  kPa,  $P_{(CO + Ar)} = 10^{\circ}$ C,  $P_{cyclopentane} = 10^{\circ}$ C,  $P_{c$ 2,990 kPa, total flow = 40 mL/min at STP.

(C and D) CO conversion and products distribution (C), and the H/C ratio of alkane feedstocks and products (D) for the coupling conversion of *n*-hexane, *n*-pentane, and *n*-butane with CO. Reaction conditions: 0.4 g M-Z5-17, T =  $450^{\circ}$ C,  $P_{alkanes} = 24$  kPa,  $P_{(CO+Ar)} = 2,976$  kPa, total flow = 40 mL/min at STP, TOS = 1.4 h.

which might be due to two reasons: (1) the shorter n-alkane (n-butane) obtained the higher H/C (Figure 1D), which meant that more hydrogen was needed to be removed for conversion of short alkane to aromatics, accounting for the lower selectivity of aromatics and higher H/C of products for n-butane coupling reactions; (2) the reaction rate of n-alkane increased over H-ZSM-5 with the size of n-alkane, 29,30 which affected the generation of aromatics from the coupling reaction of alkanes with CO.

### Effects of zeolite topology on coupling conversion of n-pentane and CO

Different kinds of zeolites, composed of the topology of TON, FER, MFI, MWW, and BEA, were meticulously selected for the coupling conversion of *n*-pentane with CO. The X-ray diffraction patterns of these zeolites are shown in Figure S2. Although these zeolites possess different channel structures, they have similar amounts of

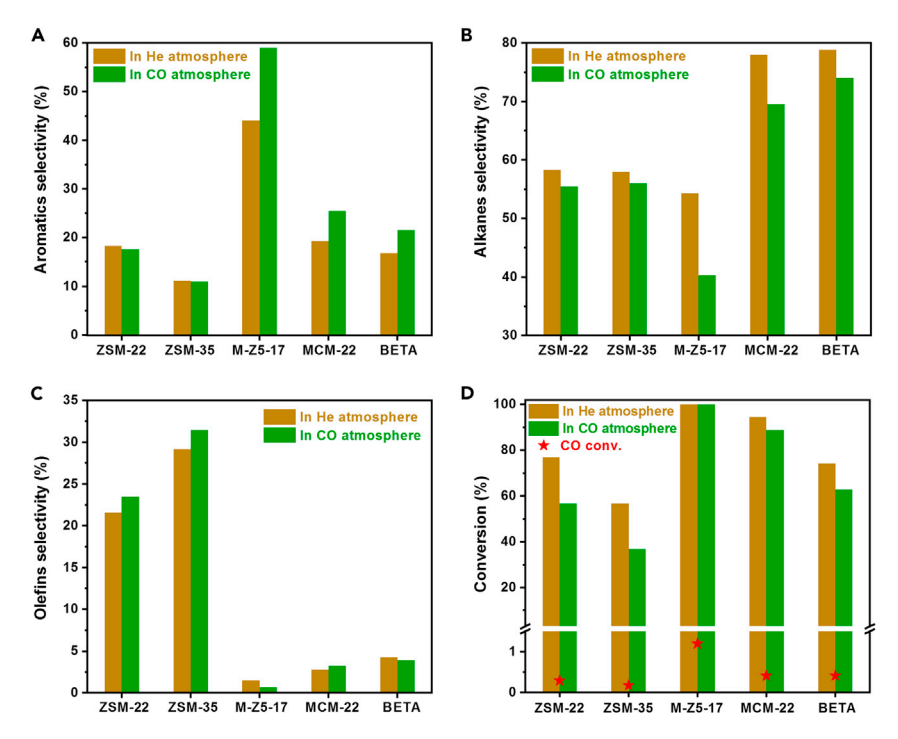


Figure 2. Catalytic performance for the conversion of n-pentane in the present of He or CO over zeolites with different topologies

- (A) Aromatic selectivity.
- (B) Alkane selectivity.
- (C) Olefin selectivity.
- (D) n-Pentane and CO conversion. Reaction conditions: 0.4 g catalyst, T = 450°C, total flow = 40 mL/min at STP,  $P_{n\text{-pentane}}$  = 24 kPa,  $P_{\text{(ICO + Ar) or He)}}$  = 2,976 kPa, TOS = 1.4 h.

acid (Table S1). The coupling reaction of *n*-pentane (a model compound of light alkanes) with CO was chosen as a model reaction. As shown in Figure 2, an increase in the aromatic selectivity and decrease in the alkane selectivity were simultaneously achieved over M-Z5-17, MCM-22, and BETA. However, a little difference of product distribution was discovered over ZSM-22 and ZSM-35, while the introduction of CO led to a significant decrease in *n*-pentane conversion over these zeolites (Figure S3), which was because a considerable amount of coke, including oxygen-containing compounds and heavy aromatics, was formed during the coupling reaction (see the analysis of retained species below), and these compounds could easily cause the channel blockage of zeolites, such as ZSM-22 and ZSM-35, with one-dimensional ten-ring channels. The highest conversion of CO and *n*-pentane was obtained over M-Z5-17, and the highest aromatic selectivity was simultaneously achieved, consistent with previous works that H-ZSM-5 was an efficient catalyst for the generation of aromatics. <sup>20,25,28</sup> Therefore, further investigations for the coupling reaction were conducted over H-ZSM-5 zeolites.

### Effects of the Si/Al ratio of H-ZSM-5 on coupling conversion of n-pentane with CO

A series of H-ZSM-5 zeolites with different Si/Al ratio was employed to investigate the effects of acid amount on the coupling reaction of *n*-pentane with CO. The XRDpatterns, Si/Al ratio, and textural properties of H-ZSM-5 zeolites are presented in Figure S4 and Table S2. While increasing the Si/Al ratio from 17 to 131, the aromatic selectivity significantly decreased, and alkane selectivity sharply increased

**Article** 



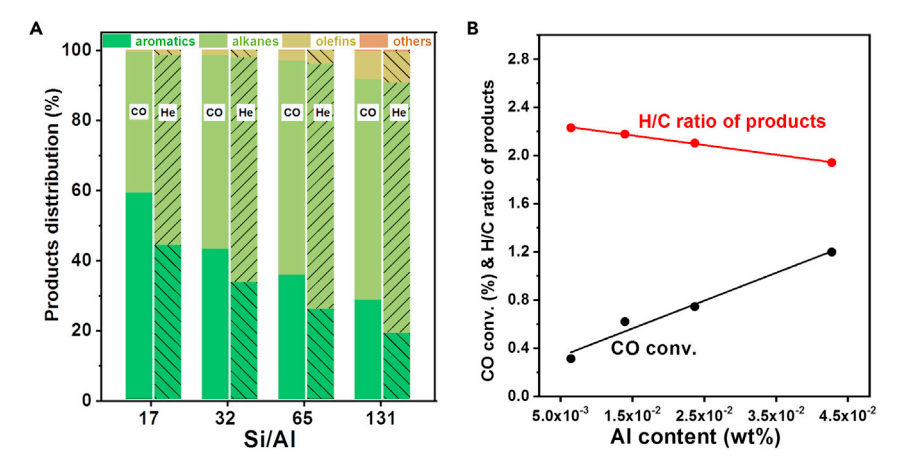


Figure 3. Catalytic performance for *n*-pentane conversion in CO and He atmosphere over H-ZSM-5 with different Si/Al ratio

(A) Contrast of products distribution.

(B) CO conversion and H/C ratio of products plotted against the aluminum content of zeolites. Reaction conditions: 0.4 g catalyst, T =  $450^{\circ}$ C, total flow = 40 mL/min at STP,  $P_{n-pentane} = 24$  kPa,  $P_{\text{(ICO + Ar) or He)}} = 2,976$  kPa, TOS = 1.4 h.

for *n*-pentane conversion in both CO and He atmospheres (Figure 3A). Compared with *n*-pentane conversion in He, the introduction of CO into *n*-pentane conversion over these H-ZSM-5 zeolites caused dramatic improvements in aromatic selectivity and decrease in alkane selectivity. As shown in Figure 3B, CO conversion increased almost linearly with increasing aluminum content of zeolites (with Si/Al ratio from 131 to 17), indicating that CO conversion was strongly dependent on the acidic sites of zeolites, consistent with carbonylation reactions.<sup>31</sup> Besides, a linear increase of CO conversion meant that more CO incorporated into products such as aromatics (discussed below), resulting in a nearly linear decrease of the H/C ratio of products.<sup>27</sup>

### Effects of reaction conditions on the coupling conversion of n-pentane with CO

Figure 4A illustrates the effects of CO partial pressure on the coupling reaction of n-pentane with CO. Increasing the CO partial pressure almost linearly increased the aromatic selectivity and decreased the alkane selectivity. Specifically, the selectivity of  $C_1$ - $C_4$  alkanes decreased simultaneously (Figure 4B), further consolidating that there existed a coupling effect between n-pentane and CO. Although the CO conversion gradually decreased, the amount of converted CO (CO conversion x mole number of CO) increased with increasing CO partial pressure. In addition, a considerable amount of  $CO_2$  ( $\sim 30\%$  selectivity) was observed, which was generated by the water-gas shift reaction.  $^{25,27}$ 

The effects of contact time are shown in Figure 4C. A sharp decrease in alkane and olefin selectivity and an increase in aromatic selectivity (from 35% to 65%) were observed with increasing contact time. Also, prolonging the contact time was favorable to the conversion of *n*-pentane (up to 100%) and CO (from 0.22% to 1.39%). The slow increment of CO conversion with contact time indicated that CO activation on the zeolites might be the rate-determining step, consistent with other carbonylation reactions over zeolites. <sup>31,32</sup> As shown in Figure 4D, a nearly linear increase in the aromatic selectivity and decrease in the alkane selectivity were simultaneously discovered with increasing reaction temperature. The high temperature was beneficial for the CO conversion, accounting for promoting the aromatics formation. At 500°C,



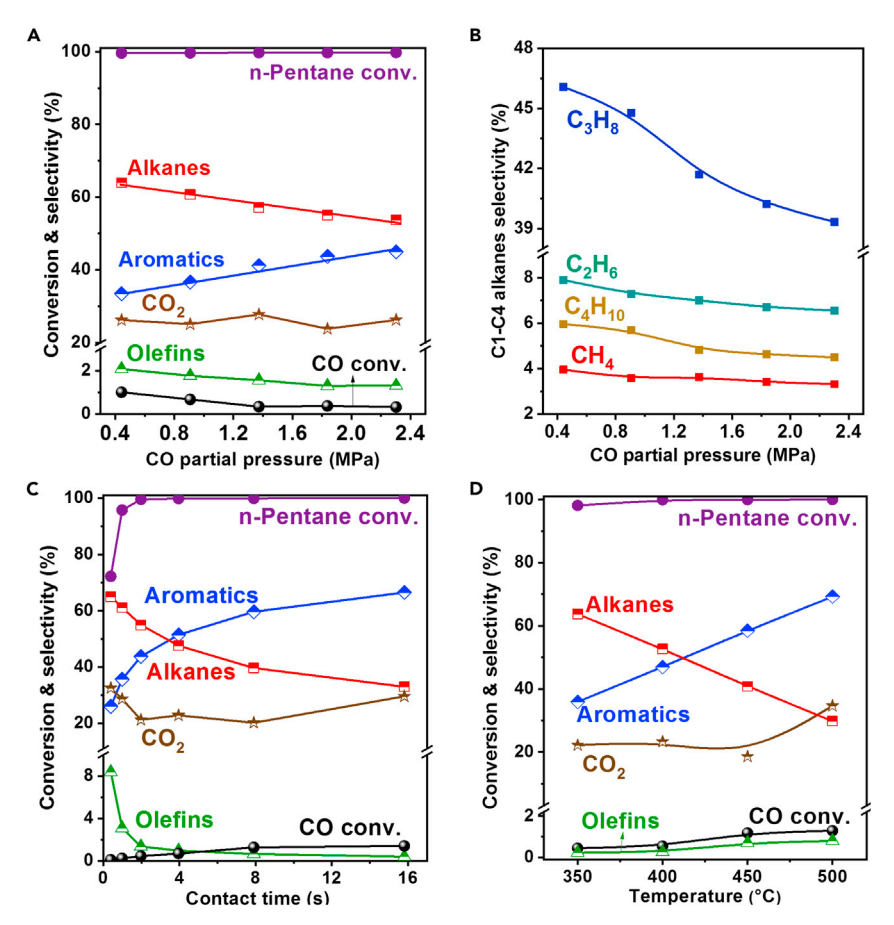


Figure 4. Effects of reaction conditions on the coupling conversion of n-pentane with CO (A and B) Effects of CO partial pressure on the conversion and selectivity (A) and  $C_1$ - $C_4$  alkane selectivity (B) for coupling reaction. Reaction conditions: 0.2 g M-Z5-17, T = 450°C, P<sub>n-pentane</sub> = 24 kPa,  $P_{(CO + Ar)} = 476-2,476$  kPa, total flow = 15.7-75.7 mL/min at STP, TOS = 1.4 h. (C) Effects of contact time on the coupling reaction. Reaction conditions: 0.002–0.8 g M-Z5-17, T =  $450^{\circ}$ C,  $P_{n-pentane} = 24$  kPa,  $P_{(CO + Ar)} = 2,976$  kPa, total flow = 40 mL/min at STP, TOS = 1.4 h. (D) Effects of reaction temperature on the coupling reaction. Reaction conditions: 0.4 g M-Z5-17,  $P_{n-pentane} = 24 \text{ kPa}$ ,  $P_{(CO\ +\ Ar)} = 2,976 \text{ kPa}$ , total flow = 40 mL/min at STP, TOS = 1.4 h.

the aromatic selectivity reached 70%, which was the highest aromatic selectivity among those reported for n-pentane conversion over acidic zeolites so far and compared favorably with catalytic performance over Zn/Ga-modified H-ZSM-5 (Table S3).

### Correlating the retained species over catalysts and aromatic selectivity

The retained species over spent catalysts were identified by GC-MS after the spent catalysts were dissolved in a hydrofluoric acid (HF) solution and extracted by CH<sub>2</sub>Cl<sub>2</sub>. As shown in Figures 5, S5, and S6, it was interestingly found that, in addition to aromatics, a considerable amount of oxygenated compounds were observed over spent M-Z5-17, mainly composed of three kinds of unsaturated ketones, including methyl-substituted cyclopentenones (ketones with one ring), methyl-substituted indanones (ketones with two rings), and fluorenones and phenalenone (ketones with three rings). Moreover, these ketones, such as methyl-substituted cyclopentenones and indanones, were observed over zeolites with different topologies (Figure S7), which could strongly adsorb on acidic sites<sup>33</sup> and block the channels of zeolites

**Article** 



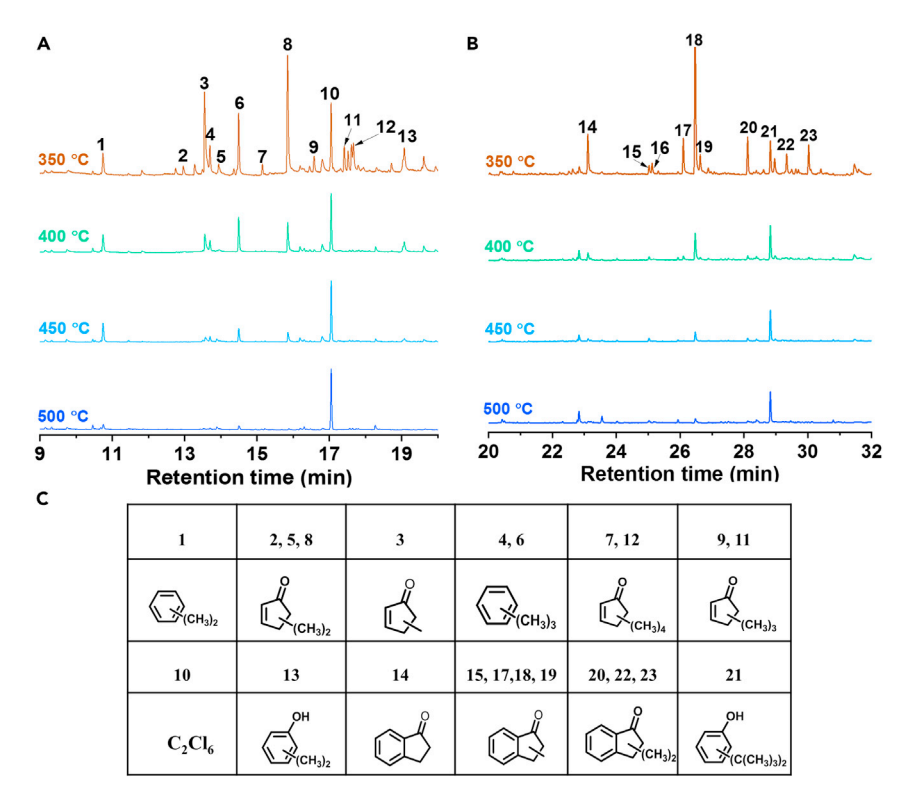


Figure 5. GC-MS results for the retained species over spent catalysts during the coupling reaction of n-pentane with CO at different temperatures

(A and B) FID signals of GC-MS with retention time of up to 20 min (A) and from 20 to 32 min (B). (C) Structures of these organic compounds marked as the corresponding number. PS: ketones with one ring include compounds marked as 2, 3, 4, 5, 6, 7, 8, 9, and 11; ketones with two rings include compounds marked as 14, 15, 17, 18, 19, 20, 22, and 23; ketones with three rings include compounds marked as 25, 26, 27, 28, and 33 (see Figure S5).

with one- or two-dimensional pore structure, such as ZSM-22 and ZSM-35, accounting for the decrease in *n*-pentane conversion during the coupling reaction. This was the first detection of methyl-substituted indanones and fluorenones and phenalenone during CO conversion over zeolites.

Detailed analysis of GC-MS results by comparing the peak area of oxygenated compounds to that of internal standard ( $C_2Cl_6$ ) revealed the evolution of different oxygenated compounds under various reaction conditions. As shown in Figure 6A, the amount of these ketones with one, two, and three rings increased almost linearly with increasing CO partial pressure from 0.5 to 2.5 MPa, demonstrating these ketones formation might be related to CO. Figure 6B shows that the amount of the ketones with three rings increased with the increasing temperature (from 350°C to 500°C), while ketones with one and two rings gradually decreased. However, these ketones were not detected in the exhausted products during the coupling reaction. These results demonstrated the ketones with one and two rings might undergo further transformation over M-Z5-17.

Furthermore, the total amount of coke increased with CO partial pressure, and first increased and then decreased with increasing the reaction temperature (350°C–500°C) (Figure S8), demonstrating that the coke generated at 350°C could undergo further conversion. Basically, the lower H/C coke components, such as compounds with multiple rings, are burned at a higher temperature ( $T_{\rm G,max}$ ). As shown in



# Chem Catalysis Article

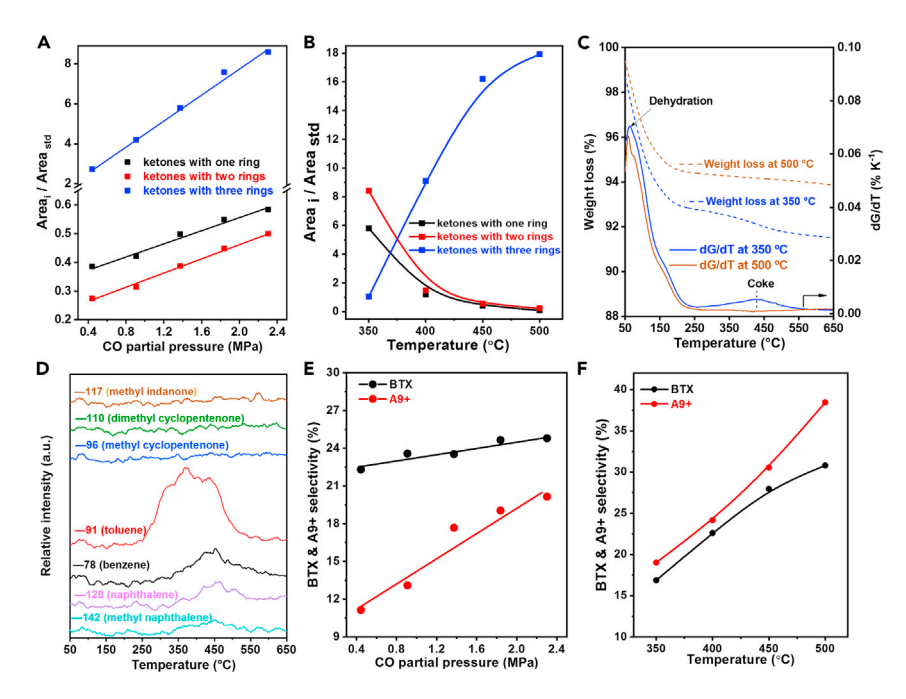


Figure 6. The retained species over spent catalysts and aromatic selectivity under different reaction conditions

- (A) Effects of CO partial pressure on the ketones with one, two, and three rings occluded in the spent M-Z5-17.
- (B) Effects of reaction temperature on the ketones with one, two, and three rings occluded in the spent M-Z5-17.
- (C) TG analysis of the spent zeolite for the coupling reaction at 350°C and 500°C along with dG/dt curves ( $50^{\circ}$ C– $650^{\circ}$ C,  $5^{\circ}$ C/min, 100 mL/min N<sub>2</sub>).
- (D) TG-MS analysis of the spent zeolite for the coupling reaction at  $350^{\circ}$ C.
- (E) Effects of CO partial pressure on BTX and  $A_{9+}$  aromatic selectivity.
- (F) Effects of reaction temperature on BTX and  $A_{9+}$  aromatic selectivity.

Figure S8C, the  $T_{G,max}$  for the spent zeolite increased with reaction temperature, indicating that the coke species gradually became larger. These results were in good agreement with the GC-MS results.

To verify the above deduction that ketones could undergo transformation over H-ZSM-5, the spent catalysts at reaction temperatures of 350°C and 500°C were heated in a He atmosphere (from 50°C to 550°C, and 5°C/min), and online-MS was applied to analyze the outgas. The spent catalyst at 350°C showed a weight loss peak in the temperature range of 300°C-550°C (Figure 6C), while the spent catalyst with a reaction temperature at 500°C had little weight loss in this temperature range. The comparison of GC-MS results of retained species before and after the temperature-programmed treatment of the spent catalyst demonstrated that the ketones with one and two rings occluded in spent zeolite at 350°C almost completely disappeared (Figure S9A). However, ketones with one and two rings were not detected by online-MS in the outgas (Figure 6D), demonstrating that these ketones, strongly adsorbed on the Brønsted acid sites, 33 did not escape from zeolite after temperature-programmed treatment (30°C-550°C, 100 mL/min He) but underwent transformation over H-ZSM-5. Moreover, the MS signal of aromatics, such as benzene, toluene, naphthalene, and methylnaphthalene, were detected in the temperature range from 300°C to 550°C, indicating that these ketones could convert into aromatics. As for the spent catalyst at 500°C, the peaks attributed to the ketones with three rings occluded in spent zeolite at 500°C barely decrease (Figure S9B),

**Article** 



revealing the weak transformation ability of these compounds accounting for catalyst deactivation.

To study the process of the ketones to aromatics, further analysis of the distribution of aromatics for the coupling reaction (Figure 6E) revealed that BTX and  $A_{9+}$  aromatic selectivity increased almost linearly with increasing the CO partial pressure, suggesting that CO might incorporate into BTX and the  $A_{9+}$  aromatics through oxygenated intermediates, such as ketones with one and two rings, verified by TG results. It has been reported that methyl-substituted cyclopentenones (ketones with one ring) mainly transformed into monocyclic aromatics,  $^{33,34}$  through which a high BTX selectivity ( $\sim$ 80% fraction in aromatics) was achieved.  $^{25}$  However, a large amount of  $A_{9+}$  aromatics (40%–60% fraction in aromatics) was obtained for n-pentane coupling reaction (Figure 6F), and these  $A_{9+}$  aromatics were mainly composed of naphthalene and its homologs (Figure S9C). It is reasonable to speculate that methyl-substituted indanones (ketones with two rings) could transform into binuclear aromatics, such as naphthalene.

To corroborate the above speculation, the reaction of 5-methyl-1-indanone (IDO) was conducted over M-Z5-17 and the exhausted products were identified by GC-MS. As expected, naphthalene and methyl naphthalene were detected (Figure S10), verifying the deduction that IDO could transform into  $A_{9+}$  aromatics, such as naphthalene and its homologs, by dehydration and isomerization, through which methyl cyclopentenones could convert to aromatics. <sup>33</sup>

### Following the process of coupling conversion of n-pentane with CO by $in\ situ\ DRIFT$ and UV-vis

To follow the reaction process of coupling reaction, in situ DRIFT study was performed over H-ZSM-5 at different temperatures. As shown in Figures 7A and 7B, the bands at 3,735, 3,655, and 3,594 cm<sup>-1</sup> were attributed to Si-OH, Al-OH, and bridging hydroxyl Si(OH)Al, respectively. The bands at 3,498, and 2,950 and 2,872 cm<sup>-1</sup> were assigned to the interactions of hydrocarbons with the bridging hydroxyl groups<sup>35</sup> and physically adsorbed hydrocarbons,<sup>36</sup> respectively. A slow decrease in the intensity of negative bands at 3,498, 2,950, and 2,872 cm<sup>-1</sup> with increasing temperature (from 170°C to 350°C) demonstrated that the physical adsorbed n-pentane gradually decreased. Meanwhile, two obvious new bands at 2,976 and 2,912 cm<sup>-1</sup> attributed to the vibrations of C-H<sup>37,38</sup> appeared at 190°C, indicating that the adsorbed n-pentane transformed into carbenium ions over M-Z5-17. Importantly, a new band at 1,680 cm<sup>-1</sup> emerged at 190°C (Figure 7B), which was attributed to the C=O stretching mode of acylium cations, <sup>39,40</sup> verified by the previous work that CO could insert into carbenium ions to generate acylium ions on acid sites. 41-44 Also, the intensity of the band at 1,680 cm<sup>-1</sup> first increased and then decreased when the temperature increased from 190°C to 350°C, suggesting that these acylium ions could undergo further transformation. Moreover, the bands at 1,595 and 1,510 cm<sup>-1</sup> were attributed to aromatic carbenium ions and the cyclic coke precursor, 45-47 respectively, suggesting the generation of aromatics and coke during the coupling reaction.

Figures 7C and 7D show the results of an *in situ* UV-vis study of the coupling conversion with increasing reaction temperature, and at 350°C over prolonged time, respectively. According to the National Institute of Standards and Technology (NIST) Chemistry WebBook (Figure S11B), the peaks at 210–230 and 310–340 nm were attributed to unsaturated aldehydes/ketones ( $\pi \to \pi^*$ ) and unsaturated aldehydes/ketones ( $\pi \to \pi^*$ ). Moreover, the bands at 250–285 and 410–



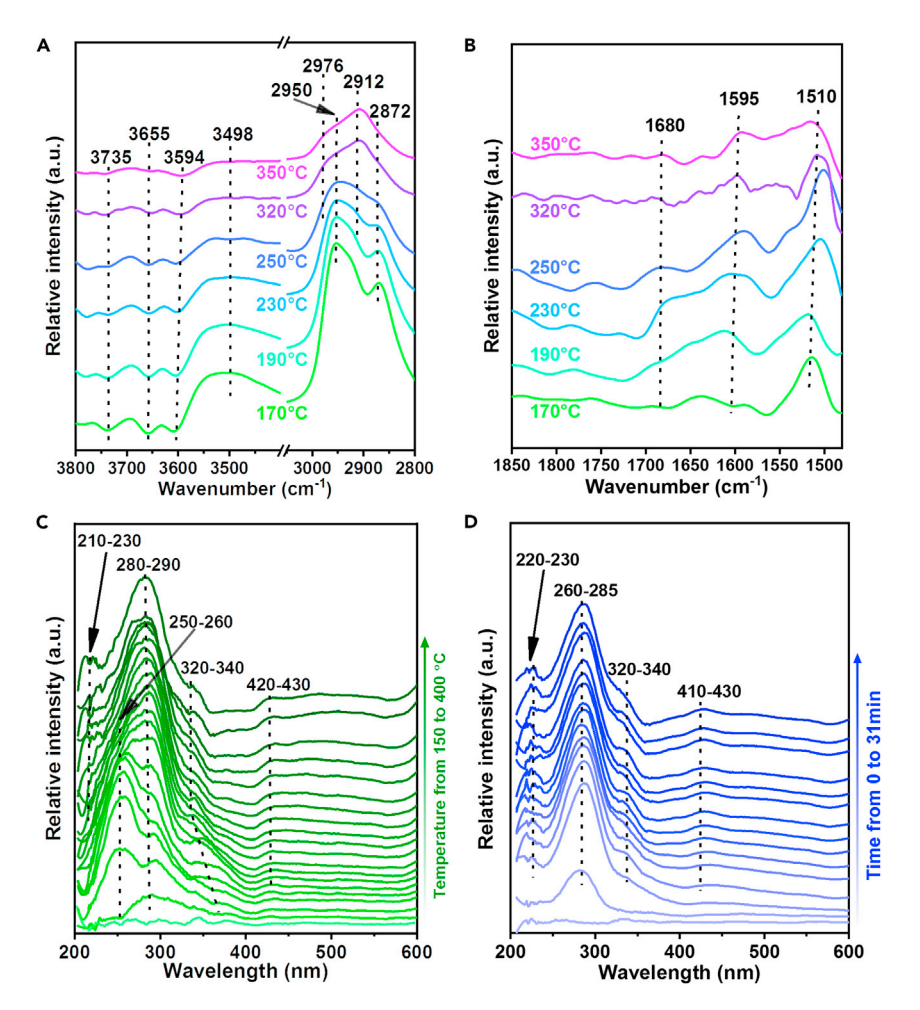


Figure 7. In situ DRIFT and UV-vis study for the coupling conversion of n-pentane and CO (A and B) In situ DRIFT spectra recorded during the coupling conversion: region of O-H and C-H (A), and region of acylium cations and coke precursors (B). (C and D) In situ UV-vis spectra recorded during the coupling reaction with increasing temperature from 150°C to 400°C (C) and prolonging time from 0 to 31 min (D).

430 nm were attributed to dienes, or neutral methylated benzenes, and polycyclic aromatics, respectively. 47–49 As shown in Figure 7C, the peaks attributed to unsaturated aldehydes/ketones (210–230 and 320–340 nm) were gradually formed with increasing reaction temperature, which might be produced from acylium ions 43 and was in good agreement with GC-MS results, which showed that a considerable amount of cyclopentenones was discovered. In addition, the new bands at 250–285 and 410–430 nm appeared, suggesting the formation of aromatics, consistent with reaction results and *in situ* DRIFT results. While the temperature was maintained at 350°C, the bands at 220–230 and 320–340 nm gradually increased with prolonged reaction time (Figure 7D), corroborating the formation of unsaturated aldehydes/ketones. The peaks at 260–285 and 410–430 nm then gradually increased, suggesting aromatic generation with reaction time.

To consolidate the above assignment, 3-methyl-cyclopenten-1-one, a compound of unsaturated aldehydes/ketones discovered in retained species, was introduced into the M-Z5-17 catalyst. As expected, bands at 220–230 and 320–340 nm occurred (Figure S11A), further corroborating that these bands were attributed to the unsaturated

Article



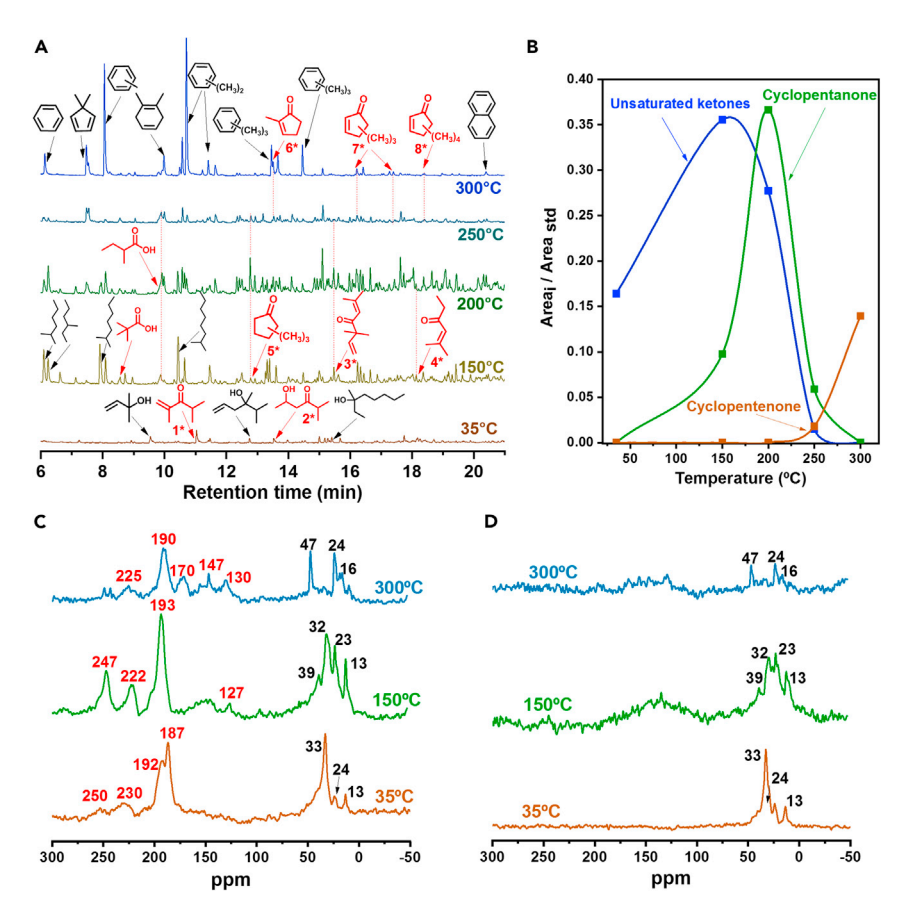


Figure 8. The co-reaction of propene with CO over M-Z5-17

(A) GC-MS results for the retained species during the co-reaction of propene with CO at different temperatures.

(B) Effects of reaction temperature on the content of unsaturated ketones (1\*, 2\*, 3\*, and 4\*), cyclopentanones (5\*), and cyclopentenones (6\*, 7\*, and 8\*).

(C and D)  $^{13}$ C MAS NMR spectra of M-Z5-17 on the co-reaction of propene with  $^{13}$ CO (C) or  $^{12}$ CO (D) at different temperatures.

aldehydes/ketones. In addition, the bands at 260-285 and 410-430 nm gradually increased with the prolonged time, demonstrating that 3-methyl-cyclopenten-1-one could convert into aromatics, consistent with previous work. 25,27,33,34,47

### Verifying the formation pathway of methyl-substituted cyclopentenones and indanones

Although methyl-substituted cyclopentenones were also discovered to be important intermediates in other reactions, <sup>25,27,33,34,47</sup> their formation mechanism remains largely unexplored. Based on the above in situ DRIFT results and previous work, 40-44 it could be speculated that acylium ions generated from CO insertion of carbenium ions might further transform into oxygenated intermediates, such as methylsubstituted cyclopentenones over zeolites. Considering that olefins easily transformed into carbenium ions over zeolites, the co-reactions of propene with CO were performed over M-Z5-17 at different temperatures (from 35°C to 300°C). As shown in Figure 8A, oxygenated compounds containing carbonyl groups were detected, which were mainly composed of acid, unsaturated ketones, methylsubstituted cyclopentanone, and cyclopentenones. Furthermore, the m/z of the

Scheme 1. Mechanism proposed for methyl-substituted cyclopentenone formation over H-ZSM-5

base peak of these compounds increased by 1 when <sup>12</sup>CO switched to <sup>13</sup>CO, demonstrating that these compounds were generated from CO (Figure S12).

<sup>13</sup>C solid-state NMR results (Figures 8C, 8D, and S13A) showed that, compared with propene conversion in <sup>12</sup>CO or He, the introduction of <sup>13</sup>CO into propene conversion caused the appearance of peaks at 170–250 ppm, which were assigned to the carbonyl group, further corroborating that these peaks were related with CO. In detail, three peaks at 245, 225, and 190 ppm were clearly observed, and the assignments of these peaks are shown in Table S4. The adsorption of 3-methyl-cyclopenten-1-one over M-Z5-17 resulted in the appearance of the signal at 224 ppm (Figure S13B), suggesting that this signal was attributed to unsaturated ketones; and, according to GC-MS results and previous literature, the peaks at 245 and 190 ppm could be assigned to methyl-substituted cyclopentanone and acid, respectively. Moreover, the signals at 130 and 147 ppm assigned to monocyclic aromatics, such as BTX and polyaromatic hydrocarbons, <sup>50</sup> were detected, indicating that CO was finally incorporated into aromatic products. In addition, the signals at 0–50 ppm were assigned to alkyl groups or/and paraffins, <sup>51</sup> and those at 187 and 170 ppm might be attributed to <sup>13</sup>CO<sup>42,43</sup> and formate species, <sup>41,42</sup> respectively.

To study the evolution of oxygenated compounds, the peak area of oxygenated compounds (in GC-MS results) compared with that of internal standard ( $C_2Cl_6$ ) was calculated (Figure 8B). Only unsaturated ketones could be detected at 35°C and the amount of these ketones decreased with increasing temperature, while methyl-substituted cyclopentanone sharply increased. Furthermore, methyl-substituted cyclopentenones gradually increased with a decrease in methyl-substituted cyclopentanone, when the reaction temperature increased from 200°C to 300°C. These results indicated that unsaturated ketones could transform into methyl-substituted cyclopentanone by cyclization, further converting into methyl-substituted cyclopentenones by hydrogen transfer.

Based on these results of propene and CO co-reaction, the formation mechanism of important intermediates (methyl-substituted cyclopentenones) was proposed and shown in Scheme 1. At low temperature (35°C), propene adsorbed on H-ZSM-5 and formed isopropyl carbenium ions, which trapped CO to generate acylium cations. <sup>40,41</sup> Then acylium cations could react with propene to generate unsaturated ketones termed 1 and 2 (compound 2 was generated from the reaction of unsaturated



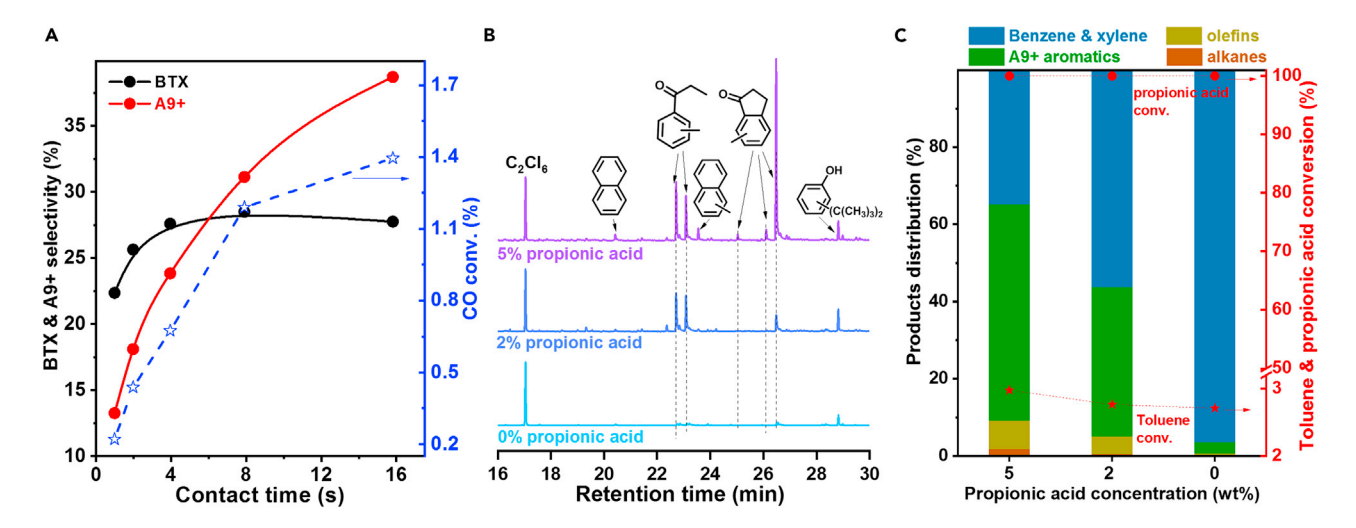


Figure 9. The aromatics selectivity during the coupling reaction and the co-reaction of toluene with propionic acid over M-Z5-17

(A) Effects of reaction contact time on the BTX and A<sub>9+</sub> aromatic selectivity and CO conversion during the coupling reaction of *n*-pentane with CO.

(B) GC-MS results for the retained species over spent zeolite (retention times of up to 30 min) during the conversion of toluene with different concentration of propionic acid.

(C) Catalytic performance for the conversion of toluene with different concentration of propionic acid over M-Z5-17. Reaction conditions:  $T = 400^{\circ}$ C, WHSV = 0.29 h<sup>-1</sup>, carrier gas (He) = 30 mL/min at STP, P = 1 bar, TOS = 2.3 h.

ketones with water). When the reaction temperature increased to 150°C, various carbenium ions could be produced by oligomerization and cracking of propene, and converted into acylium cations by carbonylation, which transformed into unsaturated ketones by Friedel-Crafts acylation of alkenes. These unsaturated ketones cyclized to methyl-substituted cyclopentanones resulting in the generation of methyl-substituted cyclopentenones.

Another important feature of coupling conversion of n-pentane and CO was that  $A_{9+}$  aromatic selectivity sharply increased with increasing contact time, even when BTX selectivity decreased at long contact time from 7.5 to 16 s (results shown in Figure 9A). This meant that BTX could further transform into  $A_{9+}$  aromatics, and a long contact time benefited the formation of  $A_{9+}$  aromatics. Moreover, CO conversion kept increasing with prolonged contact time, even at a longer contact time of 7.5 s, indicating that CO might participate in the transformation of BTX to  $A_{9+}$  aromatics. Based on the mechanism proposed in Scheme 1, this could be further extended to the reaction of acylium ions and BTX to form  $A_{9+}$  aromatics. To verify this speculation, co-feeding experiments of toluene with propionic acid, prone to form propionyl cation by dehydration,  $^{52}$  were performed over M-Z5-17.

Interestingly, oxygenated compounds, such as methyl propiophenones and indanones, were detected over the spent catalyst (Figure 9B), which corroborated the speculation that the acylium ions could react with aromatics to generate acylated aromatics over acidic zeolites, known as Friedel-Crafts acylation of arenes.  $^{53-57}$  Thus, methyl indanones could be generated from acylated aromatics by cyclization over zeolite.  $^{54,58,59}$  The introduction of propionic acid at low concentration could significantly enhance formation of  $A_{9+}$  aromatics in the products (Figure 9C) and coke, although the toluene conversion was low (<5%), indicating the rapid generation of methyl indanones, which caused the formation of  $A_{9+}$  aromatics. The reaction path of toluene conversion with propionic acid is shown in Scheme 2. In addition, fluorenones and phenalenone (ketones with three rings) were also discovered (Figure S14), which might be generated from the conversion



Scheme 2. Reaction path of the conversion of toluene with propionic acid over M-Z5-17

of naphthalene with acylium ions. These results were in good agreement with the coupling reaction of alkanes with CO. This is the first time that the formation and transformation of methyl indanones in the co-conversion of alkanes with CO over zeolites was elucidated.

### Reaction mechanism proposed for synthesis of aromatics in the coupling reaction

Based on the above results, a plausible reaction mechanism of the coupling reaction was proposed (shown in Figure 10). Light alkanes were first absorbed on Brønsted acid sites, and then carbenium ions could be generated from the protonation of alkanes by Brønsted acid followed by elimination of H<sub>2</sub>/small alkanes. Also, these generated carbenium ions could also be converted into new carbenium ions through the bimolecular mechanism, and olefins cracked from alkanes could also be protonated to form carbenium ions. 60-62 Then, absorbed CO inserts into the carbenium ions to form acylium ions were observed by in situ DRIFT study. These acylium ions could react with olefins to form unsaturated ketones, converting to methylsubstituted cyclopentenones by cyclization and hydrogen transfer, which was corroborated by <sup>13</sup>C isotope tracing and <sup>13</sup>C solid-state NMR. These methylsubstituted cyclopentenones could further transform into aromatics such as BTX. Also, the generated monocyclic aromatics could react with acylium ions to form methyl-substituted indanones, accounting for the generation of A<sub>9+</sub> aromatics. Fluorenones and phenalenone (ketones with three rings) might be generated from the reaction of acylium ions with methyl-substituted naphthalenes, resulting in the deactivation of zeolite. In addition, olefins generated from cracking of alkanes could convert into monocyclic aromatics through hydrogen transfer, which could further transform into polycyclic aromatics such as naphthalene.

The coupling reaction of different light alkanes with CO might follow a similar mechanism, but different alkanes might generate various carbenium ions with different activity, which further affects the carbonylation and hydrogen transfer reactions accounting for the distributions of different products.

### Improving BTX selectivity by using nano-sized ZSM-5 and TEOS modifications

According to the proposed mechanism, a key point to improve BTX selectivity during the coupling reaction is to reduce the secondary reactions of BTX. Herein, using a small crystal of H-ZSM-5 (Figure S15; Table S5) enhanced the diffusion of BTX, while passivating the external surface acidity of H-ZSM-5 hindered the transformation of BTX on the external surfaces. As shown in Figure 11 and Table S6, over nano-sized ZSM-5, the BTX selectivity increased while the total aromatic selectivity remained at 71%. After the modifications of N-Z5 with TEOS, the BTX fraction in aromatics gradually increased and reached 68% over N-Z5×3. Meanwhile, the BTX selectivity increased to 41.7%, while the total aromatic selectivity decreased slightly. This BTX selectivity compared favorably with catalytic performance over metal modified zeolites. These results further corroborated the proposed mechanism for coupling reactions.



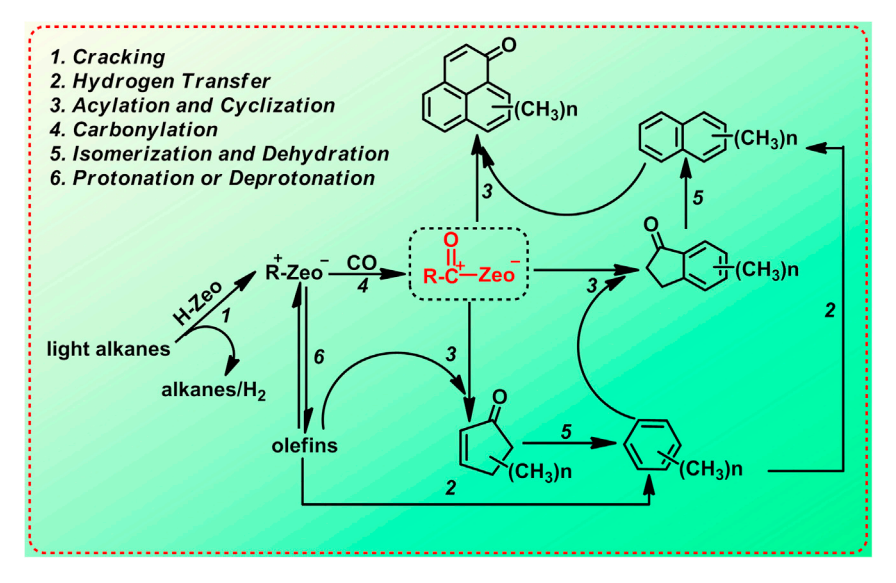


Figure 10. Reaction mechanism proposed for the formation of aromatics with high selectivity in the coupling conversion of light alkanes and CO over H-ZSM-5

#### Conclusion

In summary, a coupling effect was observed between  $C_4$ - $C_6$  alkanes and CO catalyzed by acidic zeolites, leading to a dramatic increase in the aromatic selectivity and a sharp decrease in small alkane selectivity. Effects of zeolite topologies, Si/Al ratio, reaction temperature, CO partial pressure, contact time, and different alkanes on the coupling reaction were systematically studied, and an aromatic selectivity of 85% was achieved in the case of cyclopentane and CO coupling reaction over M-Z5-17. Multiple characterizations, including in situ DRIFT and <sup>13</sup>C solid-state NMR, revealed that CO inserted into the carbenium ions generated acylium ions, and then these acylium ions could react with olefins to form unsaturated ketones, which further cyclized to methyl-substituted cyclopentanones, resulting in the formation of methyl-substituted cyclopentenones. These cyclopentenones could transform into monocyclic aromatics. Moreover, methylsubstituted indanones could be generated from the reaction of monocyclic aromatics with acylium ions, causing the formation of binuclear aromatics, such as naphthalene. In addition, ketones with three rings, such as fluorenones and phenalenone, were also found over zeolites, which had weak ability to undergo further transformation and caused deactivation of the catalyst. Based on these findings, a mechanism was proposed for the coupling reaction of light alkanes with CO. According to the proposed mechanism, using nano-sized ZSM-5 and TEOS modifications were used to improve the BTX selectivity and a high BTX selectivity of 41.7% was achieved over N-Z5×3. This provides important guidance for new routes for converting light alkanes to aromatics over zeolites.

#### **EXPERIMENTAL PROCEDURES**

### Resource availability

#### Lead contact

Further information and requests for resources should be directed to and will be fulfilled by the lead contact, Professor Zhongmin Liu (liuzm@dicp.ac.cn).

#### Materials availability

This study did not generate new unique reagents. All the chemical materials and experimental procedures are shown in the supplemental information.



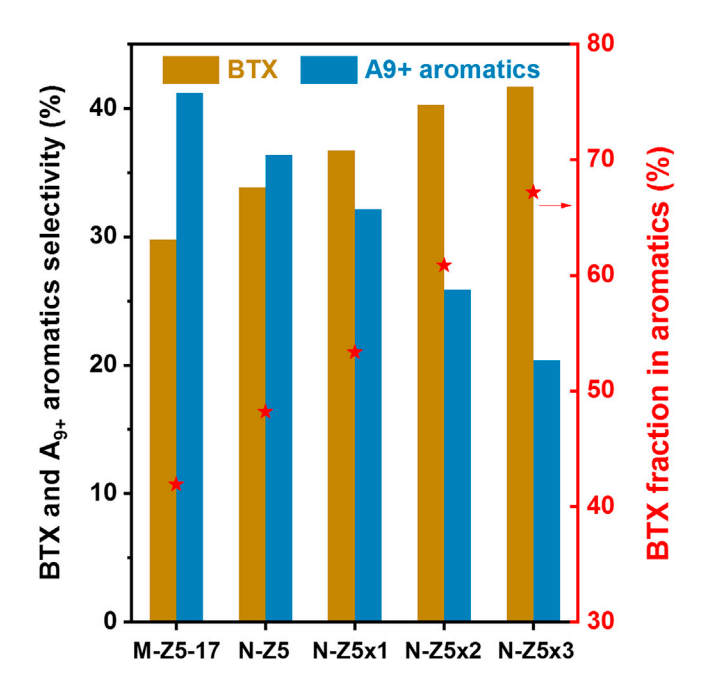


Figure 11. Distribution of aromatic products of coupling conversion over modified H-ZSM-5

Reaction conditions: 0.4 g catalyst,  $T = 500^{\circ}$ C,  $P_{n-pentane} = 24$  kPa,  $P_{(CO + Ar)} = 2,976$  kPa, total flow = 20 mL/min at STP, TOS = 1.6 h.

### Data and code availability

This study did not generate codes, software, or algorithms. All data supporting this work are available in the manuscript and supplemental information.

### SUPPLEMENTAL INFORMATION

Supplemental information can be found online at https://doi.org/10.1016/j.checat. 2021.09.004.

#### **ACKNOWLEDGMENTS**

This work was supported by the National Natural Science Foundation of China (grant nos. 21991093 and 21991090). We gratefully acknowledge Yanli He and Yijun Zheng for their assistance in catalyst characterizations.

#### **AUTHOR CONTRIBUTIONS**

C.W. performed the experiments and wrote the manuscript. K.Y. and Q.Y. discussed the experiments. S.Z. conducted the solid-state NMR experiments. C.W., J.L., and Z.L. designed the experiments, analyzed the data, and revised the manuscript. Z.L. supervised the study. All authors analyzed the results and commented on the manuscript.

### **DECLARATION OF INTERESTS**

The authors declare no competing interests.

Received: June 24, 2021 Revised: August 20, 2021 Accepted: September 8, 2021 Published: September 28, 2021

### **Article**

### CellPress

#### **REFERENCES**

- 1. Niziolek, A.M., Onel, O., Guzman, Y.A., and Floudas, C.A. (2016). Biomass-based production of benzene, toluene, and xylenes via methanol: process synthesis and deterministic global optimization. Energ. Fuel 30, 4970-4998.
- 2. Kasipandi, S., and Bae, J.W. (2019). Recent advances in direct synthesis of value-added aromatic chemicals from syngas by cascade reactions over bifunctional catalysts. Adv. Mater. 31, 18.
- 3. Settle, A.E., Berstis, L., Rorrer, N.A., Roman-Leshkov, Y., Beckham, G.T., Richards, R.M., and Vardon, D.R. (2017). Heterogeneous Diels-Alder catalysis for biomass-derived aromatic compounds. Green. Chem. 19, 3468-3492.
- 4. Ahuja, R., Punji, B., Findlater, M., Supplee, C. Schinski, W., Brookhart, M., and Goldman, A.S. (2011). Catalytic dehydroaromatization of nalkanes by pincer-ligated iridium complexes. Nat. Chem. 3, 167–171.
- 5. Zhang, F., Zeng, M., Yappert, R.D., Sun, J., Lee, Y.-H., LaPointe, A.M., Peters, B., Abu-Omar, M.M., and Scott, S.L. (2020). Polyethylene upcycling to long-chain alkylaromatics by tandem hydrogenolysis/aromatization. Science 370, 437-441.
- 6. Rahimpour, M.R., Jafari, M., and Iranshahi, D. (2013). Progress in catalytic naphtha reforming process: a review. Appl. Energ. 109, 79-93.
- 7. Davis, R.J., and Derouane, E.G. (1991). A nonporous supported-platinum catalyst for aromatization of n-hexane. Nature 349,
- 8. Xu, D., Wu, B.S., Ren, P.J., Wang, S.Y., Huo, C.F., Zhang, B., Guo, W.P., Huang, L.H., Wen, X.D., Qin, Y., et al. (2017). Controllable deposition of Pt nanoparticles into a KL zeolite by atomic layer deposition for highly efficient reforming of n-heptane to aromatics. Catal. Sci. Technol. 7, 1342-1350.
- 9. Xu, D., Wang, S., Wu, B., Zhang, B., Qin, Y., Huo, C., Huang, L., Wen, X., Yang, Y., and Li, Y (2019). Highly dispersed single-atom Pt and Pt clusters in the Fe-modified kl zeolite with enhanced selectivity for n-heptane aromatization. ACS Appl. Mater. Interfaces 11, 29858-29867
- 10. Zheng, J., Schmauke, T., Roduner, E., Dong, J.L., and Xu, Q.H. (2001). The influence of Fe on the dispersion, electronic state, sulfurresistance and catalysis of platinum supported on KL zeolite. J. Mol. Catal. A Chem. 171, 181-190.
- 11. He, P., Chen, Y., Jarvis, J., Meng, S., Liu, L., Wen, X.-D., and Song, H. (2020). Highly selective aromatization of octane over Pt-Zn/ UZSM-5: the effect of Pt-Zn interaction and Pt position. ACS Appl. Mater. Interfaces 12, 28273-28287.
- 12. Wang, S., Xu, D., Zhu, D., Zhao, B., Guan, H., Qin, Y., Wu, B., Yang, Y., and Li, Y. (2020). Elucidating the restructuring-induced highly active bimetallic Pt-Co/KL catalyst for the aromatization of n-heptane. Chem. Commun. 56, 892-895.

- 13. Liu, G., Liu, J., He, N., Sheng, S., Wang, G., and Guo, H. (2019). Pt supported on Zn modified silicalite-1 zeolite as a catalyst for n-hexane aromatization. J. Energy Chem. 34, 96-103.
- 14. Lee, K., and Choi, M. (2016). Hierarchically micro-/mesoporous Pt/KL for alkane aromatization: synergistic combination of high catalytic activity and suppressed hydrogenolysis. J. Catal. 340, 66-75.
- 15. Jarvis, J., Harrhy, J.H., Wang, A., Bere, T. Morgan, D.J., Carter, J.H., Howe, A.G., He, Q. Hutchings, G.J., and Song, H. (2020). Inhibiting the dealkylation of basic arenes during nalkane direct aromatization reactions and understanding the C6 ring closure mechanism. ACS Catal. 10, 8428-8443.
- 16. Liu, J.X., He, N., Zhou, W., Shu, M., Lin, L. Wang, J.L., Si, R., Xiong, G., Xin, Q., and Guo, H.C. (2019). Operando dual beam FTIR spectroscopy unravels the promotional effect of Zn on HZSM-5 in iso-butane aromatization. Catal. Sci. Technol. 9, 1609-1620.
- Tamiyakul, S., Sooknoi, T., Lobban, L.L., and Jongpatiwut, S. (2016). Generation of reductive Zn species over Zn/HZSM-5 catalysts for npentane aromatization. Appl. Catal. A Gen. 525, 190-196.
- 18. Liu, J., He, N., Zhou, W., Lin, L., Liu, G., Liu, C. Wang, J., Xin, Q., Xiong, G., and Guo, H. (2018). Isobutane aromatization over a complete Lewis acid Zn/HZSM-5 zeolite catalyst: performance and mechanism. Catal. Sci. Technol. 8, 4018-
- 19. Zhang, C., Kwak, G., Lee, Y.J., Jun, K.W., Gao, R., Park, H.G., Kim, S., Min, J.E., Kang, S.C., and Guan, G.F. (2019). Light hydrocarbons to BTEX aromatics over Zn-modified hierarchical ZSM-5 combined with enhanced catalytic activity and stability. Micropor. Mesopor. Mat. 284, 316-326.
- 20. Saito, H., Inagaki, S., Kojima, K., Han, Q., Yabe, T., Ogo, S., Kubota, Y., and Sekine, Y. (2018). Preferential dealumination of Zn/H-ZSM-5 and its high and stable activity for ethane dehydroaromatization. Appl. Catal. A Gen. 549, 76-81.
- 21. Bhan, A., and Nicholas Delgass, W. (2008). Propane aromatization over HZSM-5 and Ga/ HZSM-5 catalysts. Catal. Rev. 50, 19–151.
- 22. Thivasasith, A., Maihom, T., Pengpanich, S., Limtrakul, J., and Wattanakit, C. (2019). Insights into the reaction mechanism of n-hexane dehydroaromatization to benzene over gallium embedded HZSM-5: effect of H-2 incorporated on active sites. Phys. Chem. Chem. Phys. 21, 5359-5367.
- 23. Wannapakdee, W., Suttipat, D., Dugkhuntod, P., Yutthalekha, T., Thivasasith, A., Kidkhunthod, P., Nokbin, S., Pengpanich, S., Limtrakul, J., and Wattanakit, C. (2019). Aromatization of C-5 hydrocarbons over Gamodified hierarchical HZSM-5 nanosheets. Fuel 236, 1243-1253.
- 24. Xin, M., Xing, E., Gao, X., Wang, Y., Ouyang, Y., Xu, G., Luo, Y., and Shu, X. (2019). Ga substitution during modification of ZSM-5 and its influences on catalytic aromatization

- performance. Ind. Eng. Chem. Res. 58, 6970-6981.
- 25. Chen, Z.Y., Ni, Y.M., Zhi, Y.C., Wen, F.L., Zhou, Z.Q., Wei, Y.X., Zhu, W.L., and Liu, Z.M. (2018). Coupling of methanol and carbon monoxide over H-ZSM-5 to form aromatics. Angew. Chem. Int. Ed. 57, 12549-12553.
- 26. Liang, P., Zhang, Y., Wei, A., Wang, X., and Liu, T. (2015). Cracking characteristics of simulated dust-containing coal pyrolysis volatiles over regenerated nickel-based catalysts. Energ. Fuel 29, 70-77.
- 27. Wei, C., Yu, Q., Li, J., and Liu, Z. (2020). Coupling conversion of n-hexane and CO over an HZSM-5 zeolite: tuning the H/C balance and achieving high aromatic selectivity. ACS Catal. 10, 4171–4180.
- 28. Olson, D.H., Kokotailo, G.T., Lawton, S.L., and Meier, W.M. (1981). Crystal-structure and structure-related properties of ZSM-5. J. Phys Chem. 85, 2238-2243.
- 29. Narbeshuber, T.F., Vinek, H., and Lercher, J.A. (1995). Monomolecular conversion of light alkanes over H-ZSM-5. J. Catal. 157, 388-395.
- 30. Bhan, A., Gounder, R., Macht, J., and Iglesia, E. (2008). Entropy considerations in monomolecular cracking of alkanes on acidic zeolites. J. Catal. 253, 221–224.
- 31. Bhan, A., Allian, A.D., Sunley, G.J., Law, D.J., and Iglesia, E. (2007). Specificity of sites within eight-membered ring zeolite channels for carbonylation of methyls to acetyls. J. Am. Chem. Soc. 129, 4919-4924.
- 32. Celik, F.E., Kim, T.-J., and Bell, A.T. (2009). Vapor-phase carbonylation of dimethoxymethane over H-faujasite. Angew. Chem. Int. Ed. 48, 4813-4815.
- 33. Liu, Z., Dong, X., Liu, X., and Han, Y. (2016). Oxygen-containing coke species in zeolitecatalyzed conversion of methanol to hydrocarbons. Catal. Sci. Technol. 6, 8157-8165.
- 34. Ni, Y., Zhu, W., and Liu, Z. (2019). H-ZSM-5-Catalyzed hydroacylation involved in the coupling of methanol and formaldehyde to aromatics. ACS Catal. 9, 11398-11403.
- 35. van Bokhoven, J.A., Tromp, M., Koningsberger, D., Miller, J., Pieterse, J. Lercher, J., Williams, B., and Kung, H.H. (2001). An explanation for the enhanced activity for light alkane conversion in mildly steam dealuminated mordenite: the dominant role of adsorption. J. Catal. 202, 129-140.
- 36. Zhu, N., Wang, Y., Cheng, D.-G., Chen, F.-Q., and Zhan, X.-L. (2009). Experimental evidence for the enhanced cracking activity of n-heptane over steamed ZSM-5/mordenite composite zeolites. Appl. Catal. A Gen. 362, 26-33.
- 37. Forester, T.R., and Howe, R.F. (1987). In situ FTIR studies of methanol and dimethyl ether in ZSM-5. J. Am. Chem. Soc. 109, 5076-5082.
- 38. Hernandez, E.D., and Jentoft, F.C. (2020). Spectroscopic signatures reveal cyclopentenyl cation contributions in methanol-to-olefins catalysis. ACS Catal. 10, 5764-5782.



- 39. Blasco, T., Boronat, M., Concepcion, P., Corma, A., Law, D., and Vidal-Moya, J.A. (2007) Carbonylation of methanol on metal-acid zeolites: evidence for a mechanism involving a multisite active center. Angew. Chem. Int. Edit. 46, 3938–3941.
- 40. Luzgin, M.V., Thomas, K., van Gestel, J., Gilson, J.P., and Stepanov, A.G. (2004). Propane carbonylation on sulfated zirconia catalyst as studied by C-13 MAS NMR and FTIR spectroscopy. J. Catal. 223, 290-295.
- 41. Stepanov, A.G., Luzgin, M.V., Krasnoslobodtsev, A.V., Shmachkova, V.P., and Kotsarenko, N.S. (2000). Alkane carbonylation with carbon monoxide on sulfated zirconia: NMR observation of ketone and carboxylic acid formation from isobutane and CO. Angew. Chem. Int. Ed. 39, 3658-3660.
- 42. Luzgin, M.V., Stepanov, A.G., Sassi, A., and Sommer, J. (2000). Formation of carboxylic acids from small alkanes in zeolite H-ZSM-5. Chem. Eur. J. 6, 2368-2376.
- 43. Luzgin, M.V., Romannikov, V.N., Stepanov, A.G., and Zamaraev, K.I. (1996). Interaction of olefins with carbon monoxide on zeolite H-ZSM-5. NMR observation of the Friedel-Crafts acylation of alkenes at ambient temperature. J. Am. Chem. Soc. 118, 10890-10891.
- 44. Stepanov, A.G., Luzgin, M.V., Romannikov, V.N., Sidelnikov, V.N., and Zamaraev, K.I. (1996). Formation of carboxylic acids from alcohols and olefins in zeolite H-ZSM-5 under mild conditions via trapping of alkyl carbenium ions with carbon monoxide: an in situ 13 C solid state NMR study. J. Catal. 164, 411-421.
- 45. Demidov, A.V., and Davydov, A.A. (1994). Spectroscopic evidence for the formation of carbenium ions on H-ZSM-5 zeolites. Mater. Chem. Phys. 39, 13-20.
- 46. Kotrel, S., Rosynek, M.P., and Lunsford, J.H. (2000). Origin of first-order kinetics during the bimolecular cracking of n-hexane over H-ZSM-5 and H-beta zeolites. J. Catal. 191, 55-61.

- 47. Yang, L., Yan, T., Wang, C., Dai, W., Wu, G., Hunger, M., Fan, W., Xie, Z., Guan, N., and Li, L. (2019). Role of acetaldehyde in the roadmap from initial carbon-carbon bonds to hydrocarbons during methanol conversion. ACS Catal. 9, 6491–6501.
- 48. Ito, H., Nogata, Y., Matsuzak, S., and Kuboyama, A. (1969). Vacuum-ultraviolet absorption spectra of aliphatic ketones. Bull. Chem. Soc. Jpn. 42, 2453.
- 49. Kiricsi, I., Forster, H., Tasi, G., and Nagy, J.B. (1999). Generation, characterization, and transformations of unsaturated carbenium ions in zeolites. Chem. Rev. 99, 2085-2114.
- 50. Lashchinskaya, Z.N., Gabrienko, A.A., Arzumanov, S.S., Kolganov, A.A., Toktarev, A.V., Freude, D., Haase, J., and Stepanov, A.G. (2020). Which species, Zn<sup>2+</sup> cations or ZnO clusters, are more efficient for olefin aromatization? <sup>13</sup>C solid-state NMR investigation of n-but-1-ene transformation on Zn-modified zeolite. ACS Catal. 10, 14224-14233.
- 51. Zhang, W., Zhang, M., Xu, S., Gao, S., Wei, Y., and Liu, Z. (2020). Methylcyclopentenyl cations linking initial stage and highly efficient stage in methanol-to-hydrocarbon process. ACS Catal. 10, 4510-4516.
- 52. Wang, X., Ding, S., Wang, H., Liv, X., Han, J., Ge, Q., and Zhu, X. (2017). Conversion of propionic acid and 3-pentanone to hydrocarbons on ZSM-5 catalysts: reaction pathway and active site. Appl. Catal. A Gen. 545, 79–89.
- 53. Singh, A.P., and Pandey, A.K. (1997). Acetylation of benzene to acetophenone over zeolite catalysts. J. Mol. Catal. A Chem. 123,
- 54. De Castro, C., Primo, J., and Corma, A. (1998). Heteropolyacids and large-pore zeolites as catalysts in acylation reactions using alpha,beta-unsaturated organic acids as acylating agents. J. Mol. Catal. A Chem. 134,

- 55. Botella, P., Corma, A., Lopez-Nieto, J.M., Valencia, S., and Jacquot, R. (2000). Acylation of toluene with acetic anhydride over beta zeolites: influence of reaction conditions and physicochemical properties of the catalyst. J. Ćatal. *195*, 161–168.
- 56. Sartori, G., and Maggi, R. (2011). Update 1 of: use of solid catalysts in Friedel Crafts acylation reactions. Chem. Rev. 111, PR181-PR214.
- 57. Dejaegere, E.A., Thybaut, J.W., Marin, G.B., Baron, G.V., and Denayer, J.F.M. (2011). Modeling of toluene acetylation with acetic anhydride on H-USY zeolite. Ind. Eng. Chem. Res. 50, 11822-11832.
- 58. Sido, A.S.S., Chassaing, S., Kumarraja, M., Pale, P., and Sommer, J. (2007). Solvent-dependent behavior of arylvinylketones in HUSY-zeolite: a green alternative to liquid superacid medium. Tetrahedron Lett. 48, 5911–5914.
- 59. Sani-Souna-Sido, A., Chassaing, S., Pale, P., and Sommer, J. (2008). Behavior of arylvinylketones in zeolites: a systematic study. Appl. Catal. A Gen. 336, 101–108.
- 60. Lercher, J.A., van Santen, R.A., and Vinek, H. (1994). Carbonium ion formation in zeolite catalysis. Catal. Lett. 27, 91-96.
- 61. Wakayama, T., and Matsuhashi, H. (2005). Reaction of linear, branched, and cyclic alkanes catalyzed by Brönsted and Lewis acids on Hmordenite, H-beta, and sulfated zirconia. J. Mol. Catal. A Chem. 239, 32-40.
- 62. Kotrel, S., Knözinger, H., and Gates, B.C. (2000). The Haag–Dessau mechanism of protolyti cracking of alkanes. Micropor. Mesopor. Mat. 35-36, 11-20.
- 63. Wongnongwa, Y., Kidkhunthod, P., Sukkha, U., Pengpanich, S., Thavornprasert, K.-A., Phupanit, J., Kungwan, N., Feng, G., Keawin, T., and Jungsuttiwong, S. (2020). Local structure elucidation and reaction mechanism of light naphtha aromatization over Ga embedded H-ZSM-5 zeolite: combined DFT and experimental study. Micropor. Mesopor. Mat. 306. 110414.